AAS 18-376

DISPOSAL DESIGN FOR GEOSYNCHRONOUS SATELLITES REVISITED

Ioannis Gkolias[*] **and Camilla Colombo**[†]

draft of September 11, 2018

The orbits at geosynchronous altitude provide a valuable natural resource for the human kind. In the absence of atmospheric drag, human intervention is needed to keep the region clean of space debris. Current post-mission disposal guidelines deal efficiently with the geostationary low-inclination, low-eccentricity satellites but fail to efficiently regulate the whole region. In this work, we will revisit the problem of geosynchronous disposal orbits, trying to identify all possible mechanisms for designing effective disposal strategies. Massive numerical simulations are coupled with optimization techniques and semi-analytical modelling to achieve this goal.

INTRODUCTION

The resonant effects of Earth's tesseral harmonics on satellites at geosynchronous altitude provide a unique orbital evolution that can be exploited for important space applications. Since the beginning of the Space era, geosynchronous orbits (GEO) have been used for communication, weather forecast, navigation, imaging, etc. However, the absence of a well-known natural cleansing mechanism at this altitude, like the atmospheric drag in low earth orbits, makes the GEO region exposed to a non-negligible risk in view of the long term sustainability of Space. Human intervention is needed to keep this unique space asset clean and usable for the next generations. This was recognised from the very beginning and disposal strategies were planned and studied since the catalogued geosynchronous objects were just a few of hundred.[1] More recently, the Inter Agency Debris Coordination Committee (IADC) defined a set of mitigation guidelines for low inclined GEO spacecraft.[2]

Nowadays, according to the publicly-available two-line element sets around 1200 total objects are catalogued at a semi major axis around the geostationary value, including active spacecraft, rocket bodies and space debris. However, the disposal methods remain almost the same since the 1990s'. Many people believe that the debris situation in GEO is shorted out, but the question is up to what extend and in which timescale. As a matter of fact, the

[*]PhD, Research Fellow, Department of Aerospace Science and Technology, Politecnico di Milano, Via La Masa 34, 20156, Milano, Italy. email:ioannis.gkolias@polimi.it

[†]PhD, Associate Professor, Department of Aerospace Science and Technology, Politecnico di Milano, Via La Masa 34, 20156, Milano, Italy. email:camilla.colombo@polimi.it

use of a super-synchronous orbital graveyard is an excellent short-term solution, but the increase in the collision rates in the geosynchronous region is inevitable in the long-term. Population models predict on average 1 GEO collision in the next 150 years. This number is small compared to the approximately 10 collisions expected in LEO, but it is for sure something that we should not let it pass unnoticed. In addition, the recently discovered high area-to-mass ratio (HAMR) population of debris in geosynchronous orbits,[3] proved that parked satellites in super-synchronous orbits can also act as sources of secondary debris even without collisions. For example, deteriorating MLI foils can be detached from defunct satellites due to space weather or rotational drift, and HARM object orbits are following different natural dynamics such that they cross the geosynchronous protected region and pose a real danger to operating geostationary satellites. And finally, even from planetary defence point of view, if we keep the same rate of populating GEO, we will detectable by an equivalently advanced civilization by the year 2200.

The geosynchronous region, from a dynamical point of view, can be naturally separated into two distinct regions: the low-inclination region and the high-inclination region. In the low-inclination region, the natural evolution of orbits is stable and long-term stable graveyard orbits that can contain also secondary debris have to be found. In the high-inclination region, the third body perturbations, due to the sun and the moon, create interesting opportunities for designing re-entry trajectories. It is obvious that the single equation guideline, proposed by the IADC, is not adequate to encompass the dynamical particularities of the whole region.

In this work we revisit the problem of disposal design at geosynchronous altitude, with the aim to provide a global picture of the problem. First, using a single-averaged semi-analytical propagator[4] we perform a massive numerical investigation of the geosynchronous region. The obtained dynamical information is then fed into a disposal design scheme which seeks for the optimal graveyard/re-entry trajectory with respect to fuel consumption and dynamical properties (stability/re-entry time). The disposal manoeuvre at the end of life is modeled as two or one single impulse via the Gauss planetary equation in finite difference form and the manoeuvre sequence is optimized via global optimization. For the graveyard design, the long-term evolution of the satellite's perigee distance from the GEO protected region is considered as main parameter while for the re-entry design, the time required for the orbit to reach an atmospheric re-entry altitude of $120km$ is considered. The results are presented as Pareto fronts in the two-dimensional space of delta-v versus eccentricity variation/re-entry time.

For the re-entry design, as a second step we analyse the main effects that cause drastic eccentricity increase, such as the lunisolar perturbations, and propose methods of efficiently exploiting them. From an environmental point of view, removing a satellite from GEO is more sustainable than to parking it in a graveyard orbit. On the other hand, conditions at re-entry will be also analysed to assess the interaction of the incoming re-entering spacecraft with the low Earth orbit debris population. Finally, improved strategies for a cleaner GEO exploitation and their feasibility are discussed with the aim of drafting an improved set of GEO mitigation guidelines.

NATURAL DYNAMICS

Modelling the natural dynamics of the geosynchronous orbits is quite challenging since the orbits are not only influenced by the Earth's triaxiality through the resonant longitude angle, but also by the lunisolar perturbation through long term oscillation in eccentricity, anomaly of the perigee, inclination and right ascension of the ascending node.

In order to highlight the relevant dynamical features, we conducted a throughout numerical investigation via single-averaged long-term propagation of the orbits. In order to accomplish that we use the PlanOdyn[4] orbital propagation suite, adapted for geosynchronous propagation. The force model includes 4x4 geopotential, third body perturbations due to Sun and Moon (expanded up to fifth order in the parallax factor), solar radiation pressure under the cannonball approximation and Earth's precession effect. For the Sun and Moon position an analytical ephemeris is used. In Figure 1 we present a validation of our semi-analytical propagation over 120 years compared with a completely numerical integration of the full equation of motion with ephemerides given by the NASA SPICE toolkit.

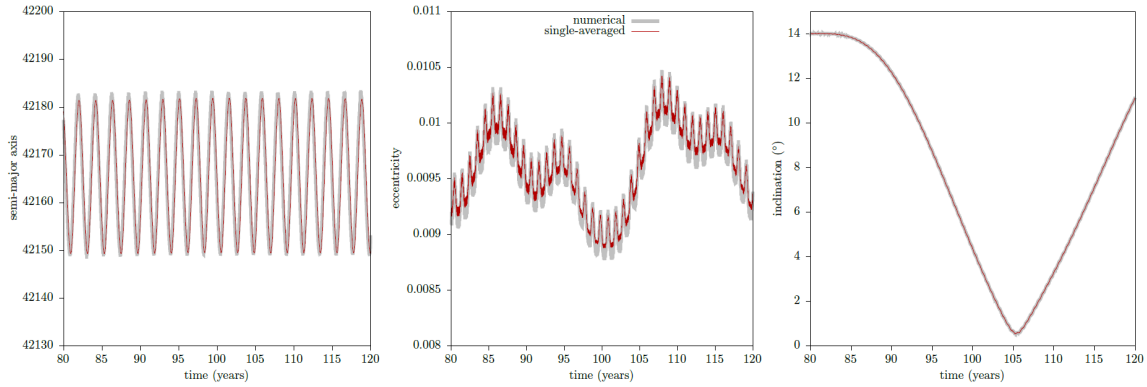

Figure 1. Comparison of the semi-analytical propagation with a fully numerical one for a geosynchronous satellite.

Since we would like to focus on the disposal properties of the orbits, we chose to characterise the evolution of each orbit via its eccentricity variation in the 120 years. Namely we employ two indicators, the classical diameter of the eccentricity

$$diam(e) = |e_0 - e_{\max}| \tag{1}$$

and a *normalised eccentricity diameter*

$$\Delta e = \frac{|e_0 - e_{\max}|}{|e_0 - e_{\text{re-entry}}|}. \tag{2}$$

The behaviour of Δe is the following: it tends to 0 when the orbit does not exhibit any significant eccentricity variations and it tends to 1 when the orbit re-enters the atmosphere. At this point we should mention that we argue against the use[5] of a chaotic indicator based on the exponential divergence of nearby orbits, like the maximum Lyapunov exponent. The reason is that along the separatrix of the geosynchronous resonance, it is known that

there exist chaotic orbits,[6] but their hyperbolicity manifests mainly as a chaotic variation of the semi-major axis and, as we will see in the following, it does not contribute in the eccentricity growth of the orbit.

For our dynamical investigation we chose three distinct mapping configurations to highlight the different dynamical features of the geosynchronous region. For each one of them we proceeded with a parametric study over the remaining feature. A total amount of more than 50 million orbits has been propagated and analysed in our work.

The first type of mapping that we studied was designed to explore the contribution of the tesseral effects on the eccentricity build up for geosynchronous orbits. The main grid is over the initial satellite semi-major axis (a) and the initial resonant angle for the geosynchronous resonance ($\lambda = \Omega + \omega + M - \theta_g$). The grid in the semi-major axis ranges from 100 km below to 100 km above the geosynchronous value ($a = 42065km$) and the resonant angle λ from 0 to 360°. In order to avoid mixing the contributions from the lunisolar and solar radiation pressure effects the resonant angle is varied through the change of M (or θ_g). The computation of the grid is repeated for a selected set of the remaining initial orbit parameters, eccentricity e and inclination i.

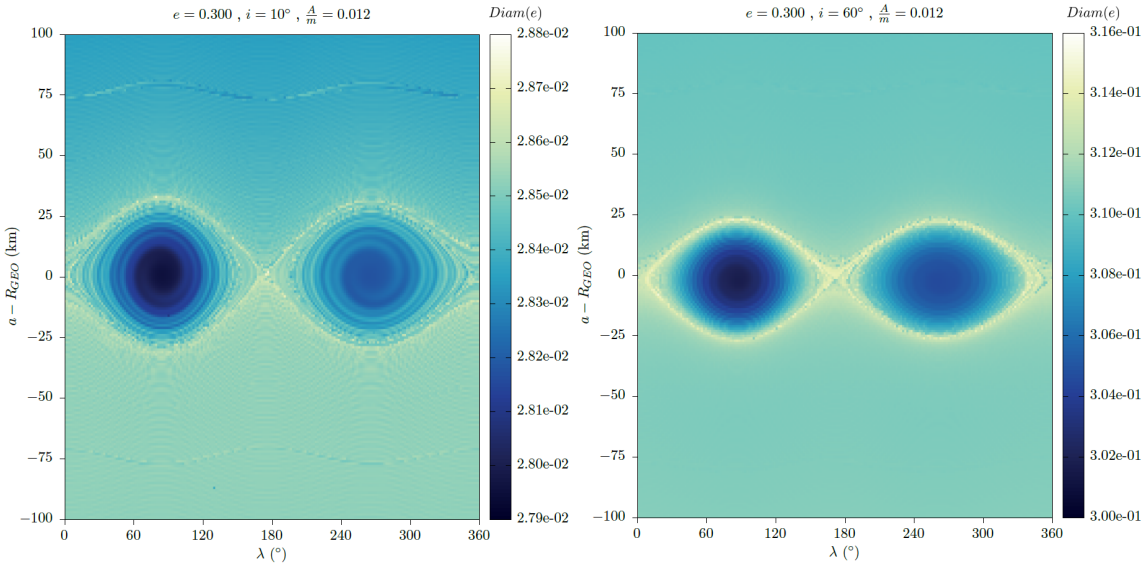

Figure 2. Dynamical map over the semi-major axis and the resonant geosynchronous angle. A low inclination $i = 10°$ (left) and a high inclination $i = 60°$ cases are presented. The initial eccentricity in both cases is $e = 0.3$. Although the separatrix of the geosynchronous resonance is clearly visible, its contribution to the eccentricity variation is insignificant.

In Figure 2 we present two of those maps for a low inclination $i = 10°$ and a high inclination $i = 60°$ case, for a quite high value of the eccentricity $e = 0.3$. As expected, the geosynchronous separatrix is clearly visible. However, placing a post-mission satellite on the separatrix does not provide any remarkable disposal opportunities. Namely, the eccentricity variation is higher along the separatrix, but only by a small, insignificant fraction with respect to the rest of the region.

The second type of maps that we have studied were designed to explore the contribution of lunisolar perturbations to distant satellite orbits and their interaction with solar radiation pressure effects. Those maps are known as *disposal maps*[7] and the main grid is over the initial longitude of the ascending node Ω and the initial argument of the perigee ω, the two orientation angles that along with the inclination i define the orientation of the orbit in space. Both angles in the grid vary from 0° to 360°. The computation of the grid is repeated for a selected set of the other initial orbit parameters (a, e, i).

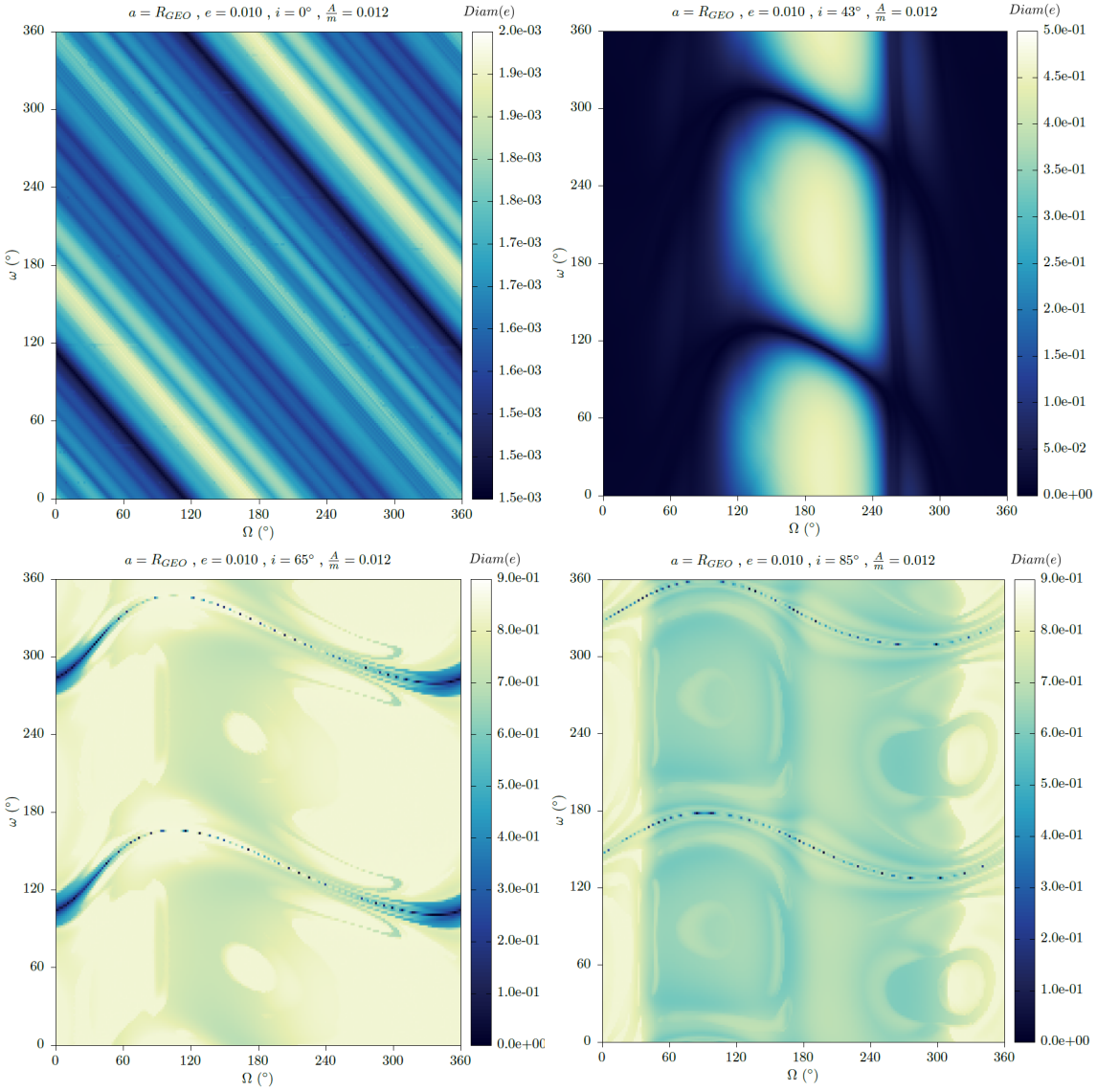

Figure 3. Disposal maps for $a = R_{GEO}$, $e = 0.01$ and inclinations of $i = 0^\circ$ (top left), $i = 43^\circ$ (top right), $i = 65^\circ$ (bottom left) and $i = 85^\circ$ (bottom right). The eccentricity variations increase significantly as we move to orbits inclined more than 40° with respect to the equator.

In Figure 3 we present a series of disposal maps for the geosynchronous semi-major axis and eccentricity of $e = 0.01$. For low inclinations $i = 0^\circ$ the eccentricity variations

are of the order of 10^{-3}, but there is a clear pattern driven mainly by the solar radiation pressure. Current disposal strategies[8,9] suggest to target at the dark spots of the map at the end of life. However, increasing the inclination changes the picture completely. The lunisolar perturbations now dictate the dynamics and create a completely different pattern. The eccentricity variations increase and they can reach values sufficient for the satellite to re-entry within the 120 years.

Finally, we present a set of action-space maps that were designed to globally scan the (a, e, i) space for regions were good graveyard or good re-entry solutions exist. The grids are set up by fixing parameters the semi-major axis and computing several maps in the $e-i$ plane for various sets of initial angles (ω,Ω and M).

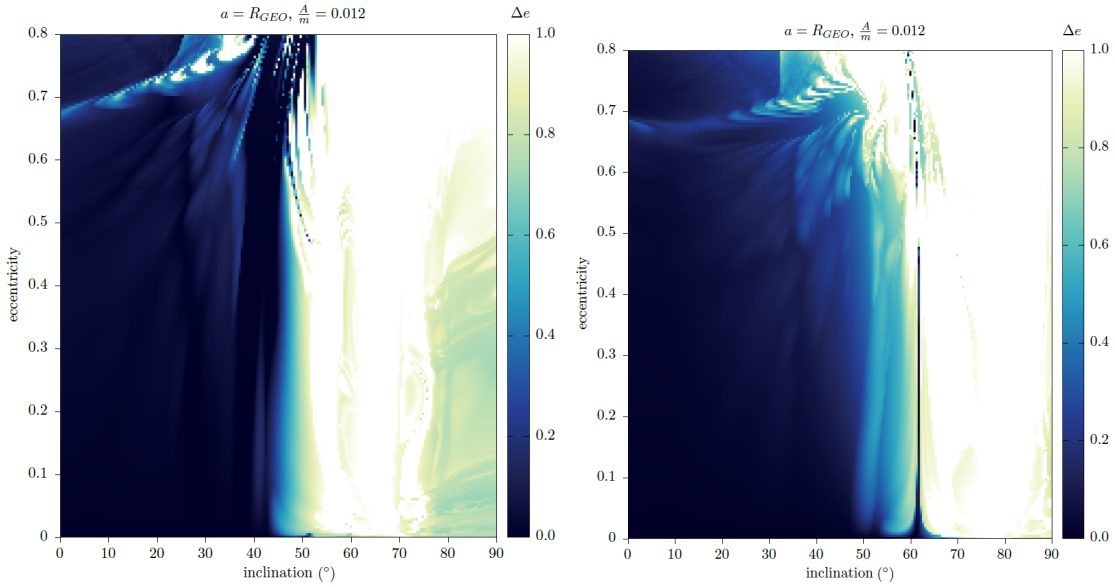

Figure 4. Dynamical maps in the (e,i)-plane. The semi-major axis is $a = R_{GEO}$ and the angles are selected randomly. For both angular configurations it is clear that there exist a natural separation in the behaviour of equatorial and inclined geosynchronous orbits.

In Figure 4 we present two cases for the e-i maps. In order to avoid the any artificial gradient due to the initial eccentricity, we use Δe as our indicator in these maps. In both cases, we see an abrupt change in orbital behaviour with respect to the inclination. On the one hand eccentricity variations are bounded for low inclinations, whereas, there is an abundance of re-entering orbits for moderate and highly inclined orbits. An interesting feature that we should mention is the existence, for particular angular configurations, of stable corridors within the unstable high-inclination domain (see the right panel in Figure 4).

Summarising our results, the natural dynamics in the orbital region about the geosynchronous altitude divide the phase space into two distinct regions. For low initial inclinations, as expected, no re-entry conditions are found; for this reason it is useful to study the total variation of eccentricity during the long-term propagation, as this can be used as a measure of the stability of the orbit, for choosing, e.g., an appropriate graveyard orbit. For

high initial inclinations, the lunisolar perturbations prevails and through the Lidov-Kozai mechanism an abundance of re-entering orbits appears, providing a significant eccentricity growth that could be exploited for disposal design. The above analysis will form the basis for the disposal manoeuvres in the next phase of this work.

DISPOSAL DESIGN

The dynamical analysis presented in the previous part will now form the basis of a disposal design tool. For a given post-mission orbit there exist three options:

- to transfer to a neighbourhood orbit which over the long term will result in a re-entry via eccentricity growth,
- to transfer to a neighbourhood orbit which will be stable over the long term,
- do not to perform any transfer and let the spacecraft orbit naturally evolve towards re-entry or towards a stable graveyard orbit.

The third option is usually not a viable solution for geosynchronous satellites, mainly due to the geosynchronous protected region*. Therefore we will concentrate in the other two options, namely the graveyard and re-entry design.

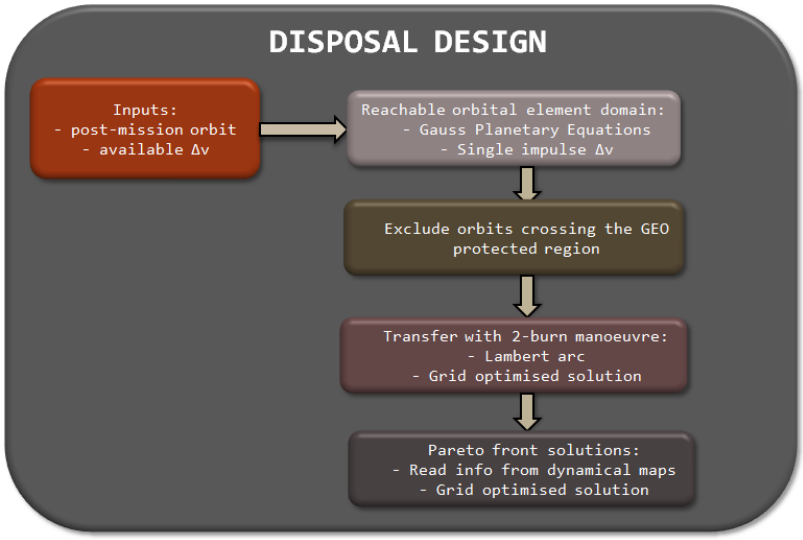

Figure 5. Flow chart of the disposal design process.

We describe now the method used for calculating the optimal disposal orbit for a given initial condition. The method developed for this work is composed of four main steps and a schematic representation of the work flow is given in Figure 5.

*The GEO protected region is defined at the synchronous semi-major axis $a_{GEO} = 42164.6935 \pm 200km$ and a latitude sector from $15°$ South to $15°$ North.

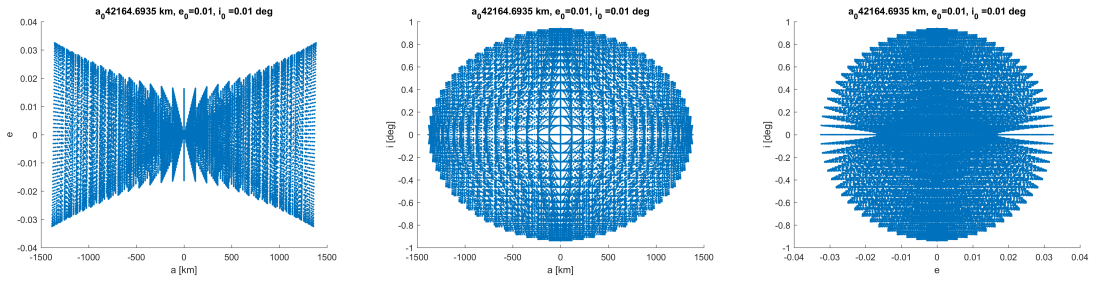

Figure 6. Reachable orbital element domain starting from an initial orbit with $a_0 = 42165$ km, $e_0 = 0.01$, $i_0 = 0.01°$, $\Omega_0 = 0°$ and $\omega_0 = 0°$.

In the first step, given a maximum available $\Delta v_{\max}$ the reachable space in orbital elements $\Delta \boldsymbol{a}$ where $\boldsymbol{a} = [a, e, i, \Omega, \omega]$ via an instantaneous impulsive manoeuvre is calculated by means of Gauss's equations written for finite differences.[10]

$$
\begin{aligned}
\Delta a &= \frac{2a^2 v}{\mu_{Earth}} \Delta v_t \\
\Delta e &= \frac{1}{v}\left(2(e + \cos f)\Delta v_t - \frac{r}{a}\sin f \Delta v_n\right) \\
\Delta i &= \frac{r}{h}\cos(f + \omega)\Delta v_h \\
\Delta \Omega &= \frac{r \sin(f + \omega)}{h \sin i}\Delta v_h \\
\Delta \omega &= \frac{1}{ev}\left(2 \sin f \Delta v_t + \left(2e + \frac{r}{a}\cos f\right)\Delta v_n\right) \\
&\quad - \frac{r \sin(f + \omega)\cos i}{h \sin i}\Delta v_h
\end{aligned}
$$

where Δv_t, Δv_n and Δv_h is the finite change in the velocity in the tangential, normal and out-of-plane direction, so that

$$
\begin{aligned}
\Delta v_t &= \Delta v_{max} \cos\alpha \cos\delta \\
\Delta v_n &= \Delta v_{max} \cos\alpha \sin\delta \\
\Delta v_h &= \Delta v_{max} \sin\alpha
\end{aligned}
$$

where $0 \leq \alpha \leq 2\pi$ and $-\pi/2 \leq \delta \leq \pi/2$ are the right ascension and the co-declination that describe the orientation of the Δv manoeuvre with respect to the $t - n - h$ frame.

The reachable domain is then defined as:

$$
\begin{aligned}
\boldsymbol{a} &= \boldsymbol{a}_0 - \Delta \boldsymbol{a} \\
\boldsymbol{a} &= \boldsymbol{a}_0 + \Delta \boldsymbol{a}
\end{aligned} \tag{3}
$$

of course removing the values which are no physically possible (e.g. $e < 0$). As an example, Figure 6 shows the shape of the reachable element domain for a circular orbit in the GEO region.

In the next step, we exclude from our reachable domain orbits that are already in the GEO protected region.

The third step consists of calculating the required Δv to reach any orbit belonging to the reachable domain (3). To this aim, the Lambert algorithm is used. A grid in time of flight for the Lambert is defined with a step of ΔToF in the domain $[0, ToF_{\text{max}}]$; given the five orbital elements on the initial orbit $\boldsymbol{a}_0$ and the target orbit $\boldsymbol{a}_{\text{target}}$, the true anomaly on the two orbits are also determined via a grid search with a step of Δf. For each point in this three dimensional grid, a Lambert arc is calculated from the initial to the target orbit and the total Δv is calculated as

$$\Delta v = ||\boldsymbol{v}_{\text{transfer}_0}(f) - \boldsymbol{v}_0(f)||$$

where the dependence on the true anomaly f is shown.

On the grid a Lambert arc is calculated for each point on the initial orbit to each point on the target orbit and the optimal transfer (i.e. the one corresponding to the minimum Δv) is stored. For a given post-mission orbit, the minimum Δv to reach each one of the reachable target orbits is stored.

The fourth and final step of our design process consists of selecting among them the best disposal strategy between re-entry or graveyard. Each target orbit corresponds to a different long term evolution, which in some cases may lead to re-entry within the 120 year time frame. To quickly characterise the long term evolution of each target orbit two parameters are used from the dynamical maps:

- the eccentricity diameter $diam(e)$
- the re-entry time.

These two parameters are used to filter and sort the best disposal. To study the two-parametric optimisation problem, the Pareto Front of the solutions $\Delta v - \Delta e$ is calculated for the graveyard disposal, while the Pareto Front of the solutions $\Delta v - \Delta t$ is calculated for the re-entry disposal. For each of the solutions belonging to the graveyard or the re-entry Pareto front the transfer characteristics are stored, i.e. Δv magnitude and direction for the Lambert arc and position on the initial and target orbit where the two impulsive Δv should be given.

As an example in Figure 7 we present a graveyard disposal design for a typical geosynchronous, equatorial and almost circular satellite. The grey points are all the computed solutions, while the red points are the solutions belonging to the Pareto Front. For a quite high initially available $\Delta v = 200\ m/s$, we see that there exist wide variety of Pareto optimal solutions. The solutions that represent the typical strategy in GEO is the one on the energetically cheapest end of the front, with a cost of about $10\ m/s$. This is the minimum required to raise the orbit outside GEO and circularise. However, we see that by spending a larger amount of fuel, even better solutions could be reached that minimise the GEO interaction with the protection region even further.

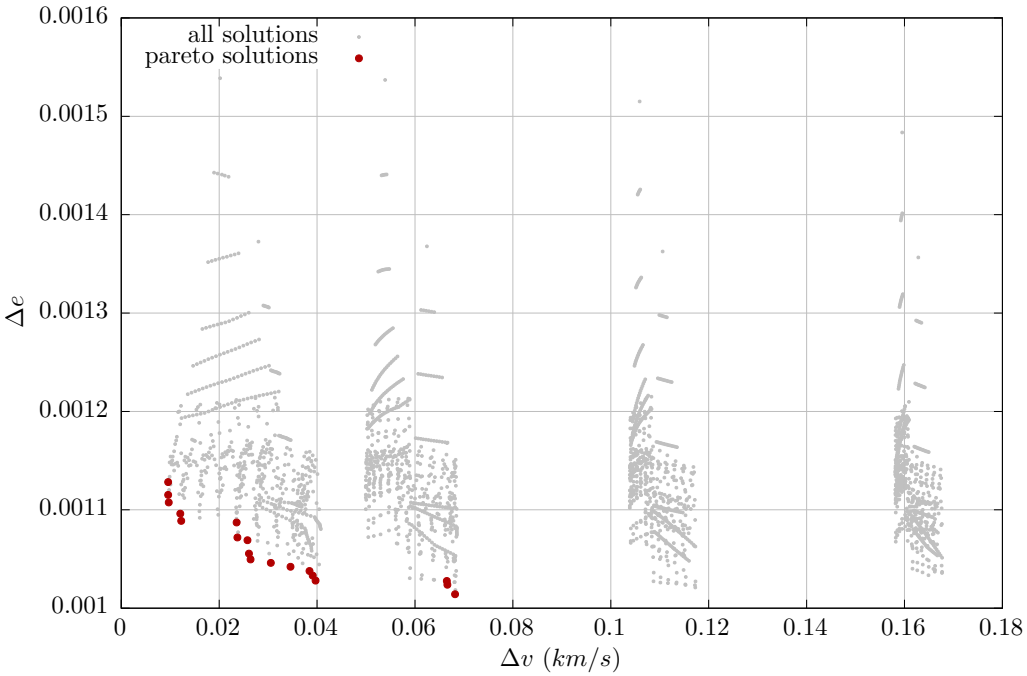

Figure 7. The Pareto front solutions for a low-inclined graveyard disposal design. The initial post-mission orbit is at geosynchronous altitude, equatorial and almost circular.

In Figure 8 we give an example of a re-entry design trajectory. The initial post-mission orbit is a hypothetical geosynchronous, highly inclined and almost circular. Like in the graveyard design plot, all the Pareto front solutions are marked with red dots, while the rest of the available solutions are denoted with grey dots. In this case, reasonable re-entry solutions with lifetimes from 30 to 65 years are reached with fuel cost that can be considered viable for many type of missions.

In Figure 9 we present a comparative study of Pareto fronts for various post-mission orbits. In the left panel, we study the case of a geosynchronous, almost circular orbits but with varying inclination. We observe that a 2° inclination provides better disposal solutions rather than a completely equatorial satellite. Moreover, increasing the inclination to 4 and 6 degrees does not improve the front, but rather lessens it. Finally, further increasing the inclination to 8° now improves the solution, an effect related to the existence of the Laplace plane[11] at 7.3° inclination. In the right panel of Figure 9, we present a series of Pareto front for highly inclined post mission orbits. For a modest post-mission Δv of 50 m/s a lot of opportunities appear for designing effective re-entry disposal trajectories with the most interesting solution appearing for 75° inclination.

At this point we can select the best disposal for any given initial orbit. Knowing the propellant on board (i.e. the maximum Δv allowed), we represent on a grid of initial conditions for the post-mission orbit, the best Δe that can be obtained or minimum Δt for re-entry, defining in such way the quality of the graveyard/re-entry orbit that can be achieved.

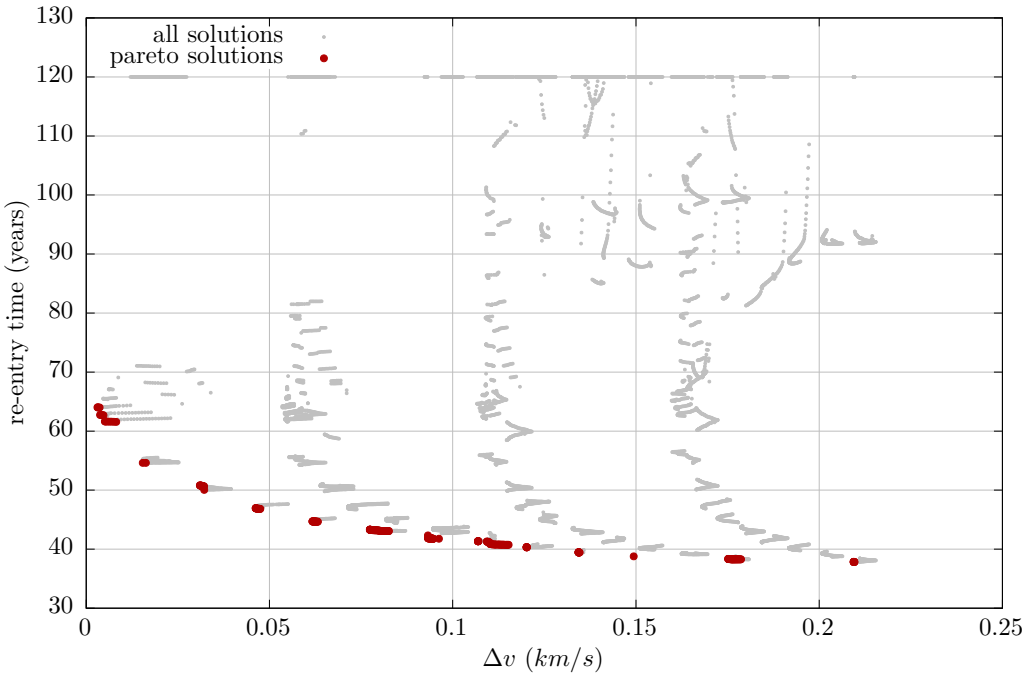

Figure 8. The Pareto front solutions for a high-inclined re-entry disposal design. The initial post mission orbit is at geosynchronous altitude, almost circular and 70° inclined with respect to the equator.

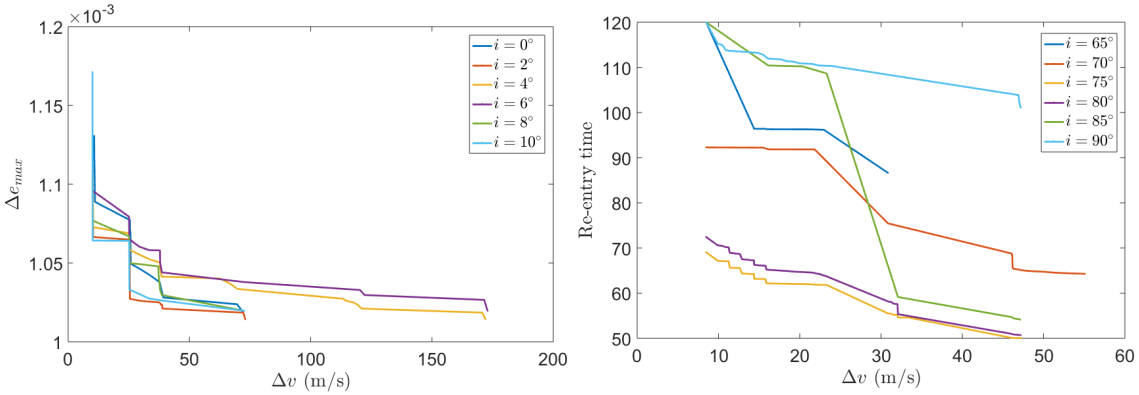

Figure 9. Pareto front solutions for different initial post-mission orbits. In the left panel: the graveyard Pareto fronts are presented for a geosynchronous, almost circular satellite and varying the post-mission inclination. In the right panel: the re-entry Pareto fronts are compared for almost circular orbits geosynchronous orbits but for high values of the inclination.

Figure 10 shows for a given value of the Δv of 80 m/s the quality of the graveyard solution that can be achieved (Δe) and the minimum Δt in the case of re-entry disposal. These solutions correspond to an initial geosynchronous $a = R_{GEO}$ post-mission orbit with $\omega = 0^\circ$ and $\Omega = 0^\circ$. Apart of the small translational region, where both re-entry and graveyard solution can be targeted, in most of the cases for initial inclination less than 60° to 65° re-entry in less than 120 years is not possible (re-entry in a longer time period

could be achieved but this has not been analysed), and for inclination higher than 60° to 65° re-entry can be achieved with a minimum time of about 40 years. Conversely, the quality of the graveyard orbit decreases with the increase of the initial inclination, showing much larger eccentricity variations that render those orbits unusable as graveyards.

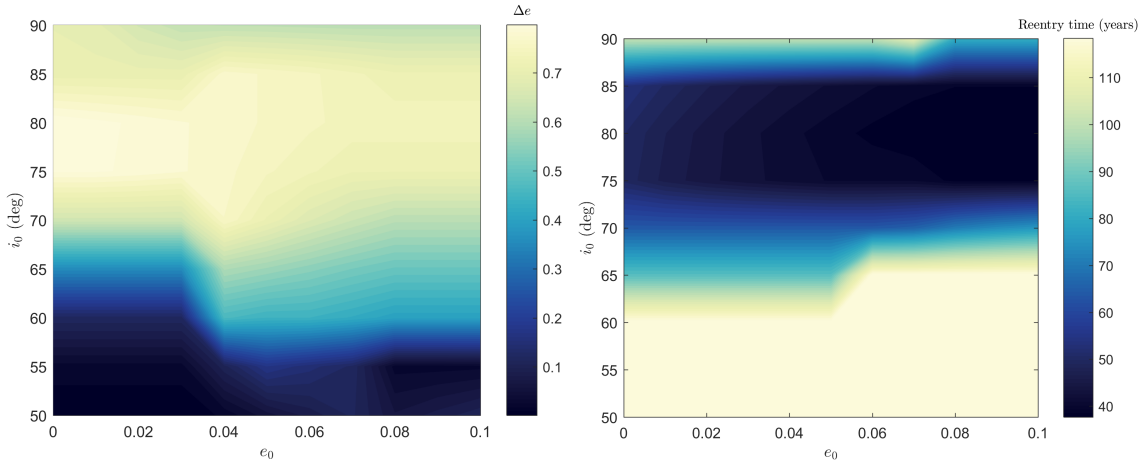

Figure 10. Best case disposal design maps for highly inclined geosynchronous orbits with a post-mission Δv of about $80\ m/s$. Surpassing an inclination value of about 60°, there is a transition from a region where the graveyard solutions are best to the a region where the re-entry solution prevail.

DISPOSAL ISSUES

In the discussion about the natural dynamics separation of the geosynchronous region, we mentioned the abundance of re-entering orbits. However there is an important aspect of the disposal process that we did not discuss, the timescale in which a geosynchronous satellite can re-enter. In Figure 11 we present a fast re-entering orbit from our studies. Its lifetime is less than 18 years, which makes it complaint even with 25 years rule that is imposed in LEO. Moreover, its interaction with the GEO protected ant the LEO protected regions is minimal, thus it's collision probability is one order of magnitude less than a 25 year rule complaint LEO satellite. In order to check that this kind of evolution is real and not an artefact of our semi-analytical scheme, we compare the time-evolution with a fully numerical propagation.

However, such short-lived orbits do not come as a surprise to people that are working with distant and inclined satellites.[12–14] In Figure 12 we present a typical disposal map, but this time we use the orbital lifetime as colormap, instead of the eccentricity diameter. We see that there is whole patch of short lived orbits between 200° and 260° of the satellite's RAAN.

Trying to identify the interesting properties of those orbits we select a set of 12 orbits with same initial conditions except for the node, which is sampled every 30° along the grey line in Figure 12. The orbits belonging to the fast-re-entering patch are colorcoded red. In Figure 13 we present the orbital evolution of those orbits. The eccentricity evolution

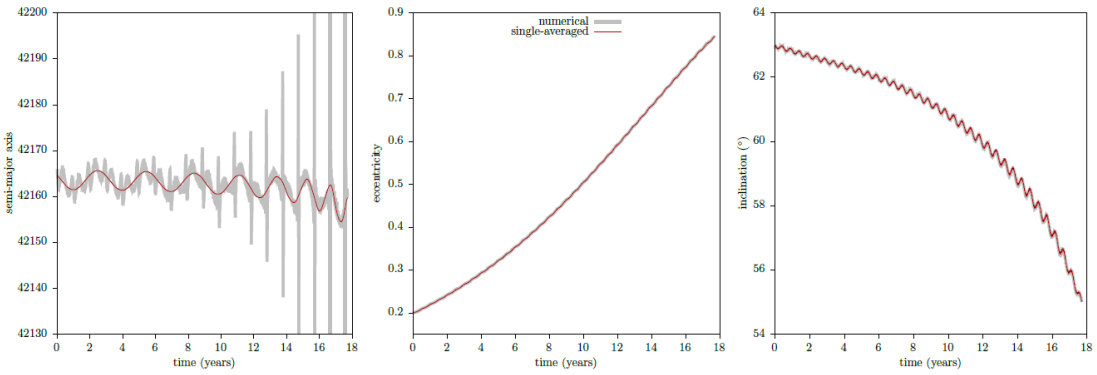

Figure 11. Time evolution of fast re-entering orbit from high inclined GEO region. The semi-analytical propagation is one more time compared with a fully numerical result to confirm the existence of such short-lived orbits.

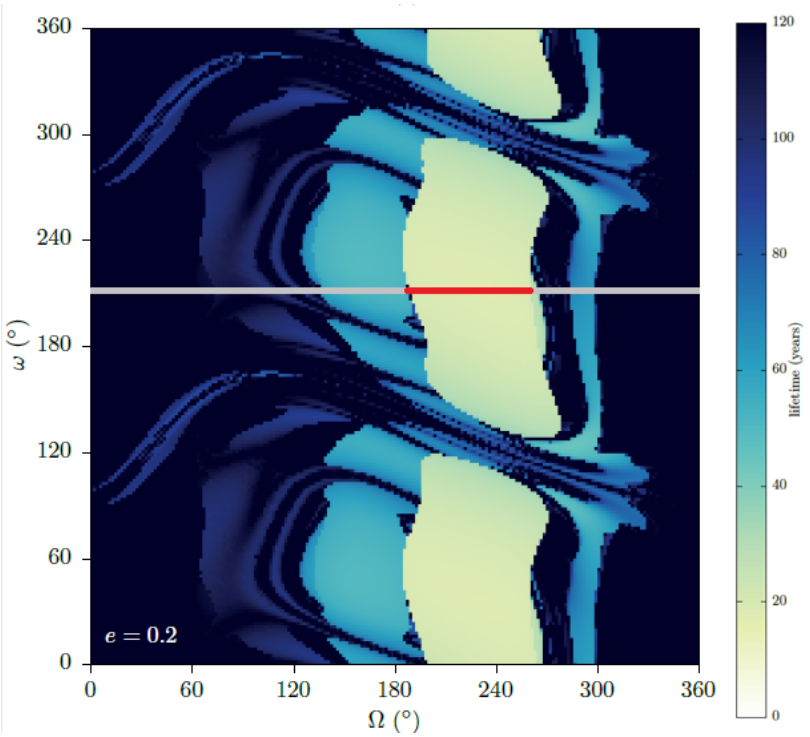

Figure 12. Disposal map for inclination $a = R_{GEO}$, $e = 0.2$ and $i = 63°$. The colomap corresponds to the orbital lifetime of the orbits. An interesting patch of short-lived orbits appears between a RAAN of $200°$ and $260°$

as well as the evolution in the $(e\cos(\omega), e\sin(\omega))$ plane gives some hints of the cleansing mechanism. The fast re-entering orbits are just orbits that reach the re-entry limit within the first quarter in of the evolution under the Lidov-Kozai type of dynamics.

Finally, we would like to draw some attention to the case of the Sirius constellation. This constellation operated for more than 10 years at highly inclined and eccentric GEO orbit, providing satellite radio services for Canada. At the end of the constellation's operational life, the operators decided to follow the IADC rules and move the satellites away from

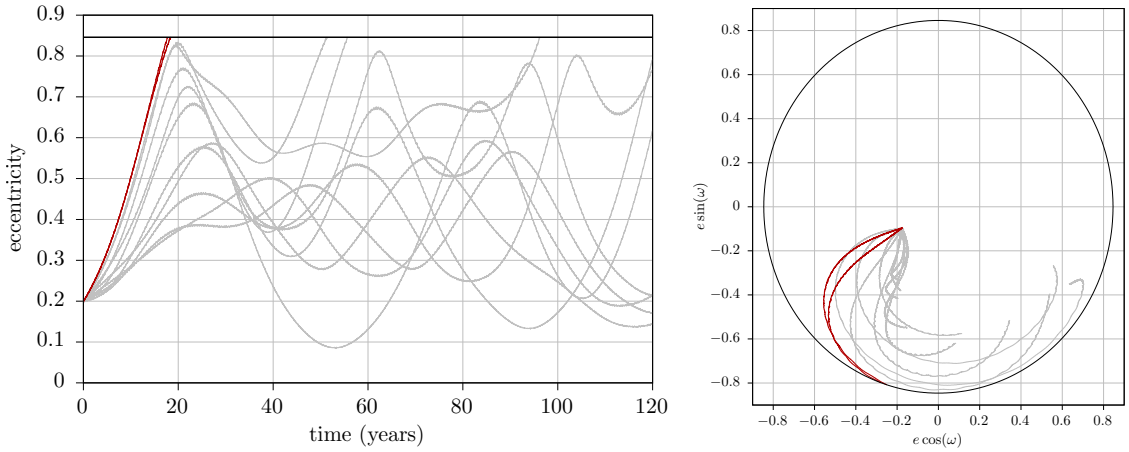

Figure 13. In the left panel: the eccentricity evolution of a set of 12 orbits with same initial condition except for node, which is sampled every $30°$. Those with $\Omega = 210° \ \& \ 240°$ have re-entry times less than 20 years (red lines). In the right panel: the same evolution in the $(e\cos(\omega), e\sin(\omega))$ plane.

GEO by circularising the orbits. However, with the same fuel amount that was spent for this operation, it is very probably that they could have reached one of the fast re-entering orbits and completely removed their satellites from near Earth space.

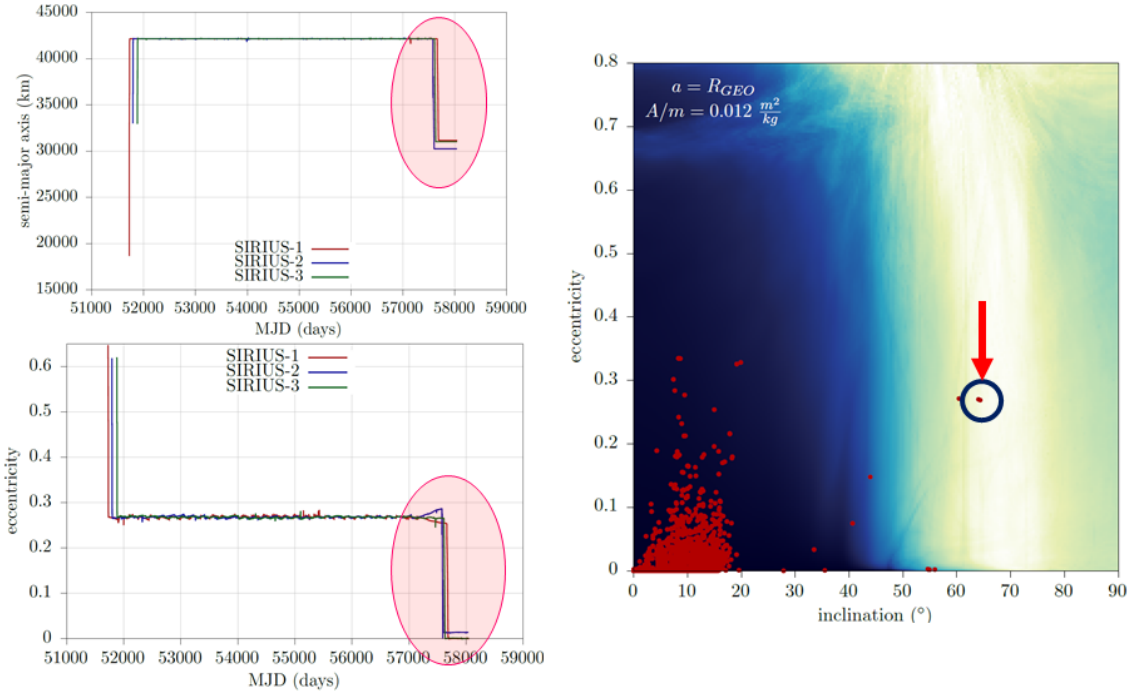

Figure 14. The case of the Sirius constellation. In the left panel: the Two Line Element history of all three components showing the end-of-life manoeuvre that was chosen from the operators. In the right panel: the natural dynamics of the geosynchronous region. The Sirius constellation was embedded in a region where an abundance of re-entry solution existed in its vicinity.

CONCLUSIONS

As a final remark, we have to notice that for low initial inclinations graveyard orbits with low variation of eccentricity are the only viable solution for GEO end-of-life disposal. However, for inclined geosynchronous satellite natural re-entry is possible within reasonable timescales. The process of disposal design is quite complicated task, and in many cases the optimal solution is case depended. Current mitigation guidelines are satisfactory for equatorial GEO, but fail to regulate the whole region. Moreover, we should start thinking of alternatives solution that could lead to a sustainable exploitation of GEO.

ACKNOWLEDGMENTS

The research leading to these results has received funding from the Horizon 2020 Program of the European Union's Framework Programme for Research and Innovation (H2020-PROTEC-2015) under REA grant agreement number 687500 – ReDSHIFT.

REFERENCES

[1] V. A. Chobotov, "Disposal of spacecraft at end of life in geosynchronous orbit," *Journal of Spacecraft and Rockets*, Vol. 27, Aug. 1990, pp. 433–437.

[2] IADC, "IADC Space Debris Mitigation Guidelines," *Inter-Agency Space Debris Coordination Committee, Revision 1*, 2007.

[3] T. Schildknecht, R. Musci, M. Ploner, G. Beutler, W. Flury, J. Kuusela, J. de Leon Cruz, and L. de Fatima Dominguez Palmero, "Optical observations of space debris in GEO and in highly-eccentric orbits," *Advances in Space Research*, Vol. 34, Jan. 2004, pp. 901–911.

[4] C. Colombo, "Planetary Orbital Dynamics (PlanODyn) suite for long term propagation in perturbed environment," *6th International Conference on Astrodynamics Tools and Techniques (ICATT)*, Mar. 2016.

[5] J. Daquin, I. Gkolias, and A. J. Rosengren, "Drift and its mediation in terrestrial orbits," *ArXiv e-prints*, Feb. 2018.

[6] S. Breiter, I. Wytrzyszczak, and B. Melendo, "Long-term predictability of orbits around the geosynchronous altitude," *Advances in Space Research*, Vol. 35, 2005, pp. 1313–1317, 10.1016/j.asr.2005.02.033.

[7] R. Armellin and J. F. San-Juan, "Optimal Earth's reentry disposal of the Galileo constellation," *Advances in Space Research*, Vol. 61, Feb. 2018, pp. 1097–1120, 10.1016/j.asr.2017.11.028.

[8] N. Delong and C. Frémeaux, "Eccentricity Management for Geostationary Satellites during End of Life Operations," *4th European Conference on Space Debris* (D. Danesy, ed.), Vol. 587 of *ESA Special Publication*, Aug. 2005, p. 297.

[9] C.-C. Chao and S. Campbell, "Long-Term Perigee Height Variations of Geo Disposal Orbits a Revisit," *4th European Conference on Space Debris* (D. Danesy, ed.), Vol. 587 of *ESA Special Publication*, Aug. 2005, p. 303.

[10] M. Vasile and C. Colombo, "Optimal Impact Strategies for Asteroid Deflection," *Journal of Guidance, Control, and Dynamics*, Vol. 31, No. 4, 2008, pp. 858–872.

[11] A. J. Rosengren, D. J. Scheeres, and J. W. McMahon, "The classical Laplace plane as a stable disposal orbit for geostationary satellites," *Advances in Space Research*, Vol. 53, Apr. 2014, pp. 1219–1228, 10.1016/j.asr.2014.01.034.

[12] I. Wytrzyszczak, S. Breiter, and W. Borczyk, "Regular and chaotic motion of high altitude satellites," *Advances in Space Research*, Vol. 40, 2007, pp. 134–142, 10.1016/j.asr.2006.11.020.

[13] A. B. Jenkin, J. P. McVey, J. R. Wilson, and M. E. Sorge, "Tundra disposal orbit study," *Proceedings of the 7th European Conference on Space Debris, April 18-21, 2017, Darmstadt (Germany)*, 2017.

[14] M.-J. Zhang, C.-Y. Zhao, Y.-G. Hou, T.-L. Zhu, H.-B. Wang, R.-Y. Sun, and W. Zhang, "Long-term dynamical evolution of Tundra-type orbits," *Advances in Space Research*, Vol. 59, Jan. 2017, pp. 682–697, 10.1016/j.asr.2016.10.016.